Data-Driven Antenna Delay Calibration for UWB Devices for Network Positioning

Zuoya Liu, Teemu Hakala, Juha Hyyppä, Antero Kukko, Harri Kaartinen, and Ruizhi Chen

Abstract— This study presents a real-time and fully automatic antenna delay calibration approach for ultrawideband (UWB) devices, which can be utilized to evaluate the combined delay of each UWB device used in the positioning system. Two estimators, a coarse estimator and a fine-tuning estimator, operate closely together in the calibration. The coarse estimator can determine a common coarse value for all devices involved in the calibration; the fine-tuning estimator continuously determines the optimal value for each device. More than three UWB devices can be calibrated simultaneously in real-time in the developed approach, making it a suitable solution for positioning applications with a large number of UWB devices. To evaluate the calibration accuracy of the proposed approach and verify the ranging accuracy and precision at different distances, experiments were conducted in an indoor office space and outdoors in an open space using universal UWB devices (DWM1001 from Decawave). The experimental results show that the proposed approach achieves a ranging precision of better than ±0.01 m within a base UWB network for each pair of devices and achieves a ranging accuracy and precision of better than ±0.05 m in a distance range from 1 to 25 m after calibration and bias correction for a remote/moving UWB device. Therefore, the developed approach is sufficient for UWB-based applications in which each UWB device must remain in a stationary state at the horizontal plane spanned by the devices in space to ensure the performance of the positioning system.

Index Terms— Antenna delay, calibration, high accuracy, network positioning, real-time and automatic, ultrawideband (UWB).

I. INTRODUCTION

TIME-OF-FLIGHT (ToF) measurement-based high-accuracy and high-precision ranging technologies are the basis and core of indoor and outdoor positioning and navigation systems due to their advantages of low complexity, high robustness, high extensibility, and adaptability compared with received signal strength indication (RSSI)-, angle-, fingerprint-, and inertial measurement unit (IMU)-based solutions [1], [2], [3], [4], [5], [6]. Based on this technique, positioning, navigation, and tracking services for mobile targets [2], such as robotics and pedestrians, in indoor and outdoor environments can easily be achieved with excellent performance in terms of positioning accuracy, scalability, real-time performance, and reliability [6].

Ultrawideband (UWB) communication, an outstanding representative of ToF technologies, has become increasingly popular in recent decades and has emerged as the most promising candidate for ubiquitous location-related applications [7]. It can achieve decimeter-level or even centimeter-level ranging, positioning, and tracking in line-of-sight (LoS) conditions by measuring the ToF of wideband pulse signals traveling between a transmitter and a receiver with subnanosecond resolution [8]. However, for UWB devices without antenna calibration, even in LoS conditions, ToF measurements are subject to ranging offsets caused by inaccurate transmission (Tx) and reception (Rx) antenna delays of the devices [9]. These offsets can severely disrupt the ranging precision between the transmitter and the receiver, thereby reducing the positioning accuracy of the system, necessitating a calibration procedure before deploying and implementing a positioning system. Moreover, the Tx and Rx antenna delays are particularly dependent on the specific devices [9], and slight differences exist from device to device [11]. These variations affect the final positioning accuracy of such systems by tens of centimeters, which hinders their use, especially for high-accuracy applications [12].

Many efforts have been made to calibrate the antenna delays of UWB devices. Decawave Ltd., presented an approach using an iterative two-way ranging (TWR)-based measurement method to determine the combined antenna delays of UWB devices [9], which can then be used to correct the Tx and Rx timestamps. Three UWB devices placed at fixed known distances were used in this approach, and TWR was performed consecutively between each pair of UWB devices.

Based on the mean of these obtained TWR measurements, the optimal delays of the three devices are determined by producing uniformly distributed candidates and altering each iteration to find a local optimum that produces the least difference between the actual and measured distances. Gui et al. [14] presented a least squares-based calibration method, which is very similar to the calibration method presented by Decawave. These two methods depend strongly on the ranging accuracy and the estimation algorithm, and any ranging errors are fed back into the calibration, resulting in inaccurate antenna Tx and Rx delays.

Horvath et al. [13] introduced a method to determine the antenna delay of a UWB device with the help of two other UWB devices, whose antenna delays do not need to be known. This method requires strict reply delay times to implement symmetric double-side TWRs, which may not be feasible for two separate UWB devices. To improve the calibration accuracy, Shah et al. [15] introduced a distance-based calibration method using three modules, and one of these modules acts as auxiliary equipment to listen to the messages transmitted by the other two modules. However, this method can only evaluate two nodes' antenna delays one time, which is not very efficient, especially for large-scale applications.

Motivated by current shortcomings and the potential demand for high-accuracy UWB-based positioning systems, this study introduces a real-time, reliable, and fully automatic calibration approach to evaluate the antenna delay of each UWB device of a positioning system. Two estimators, a coarse evaluator and a fine-tuning evaluator, work together and closely in the proposed approach. The coarse evaluator determines the same coarse delay for all UWB devices involved in the calibration by searching for the optimal delay with a binary search algorithm. The fine-tuning evaluator determines the best delay for each device by adjusting the Tx and Rx delay of each device continuously with a minimum scale of two units of time of the UWB chip. The fundamental unit of time in the UWB chip is a tick. For both evaluators, the delay set with minimum ranging errors is determined as the optimal value of the delay of the devices. Three UWB devices are necessary for the approach to construct a stable equilateral triangle; thus, the approach can calibrate three devices simultaneously, which is significant for actual applications with a large number of UWB devices.

The outline of this work can be summarized as follows. Section II describes the ToF measurement algorithm and possible sources of ranging error. Section III describes the proposed approach in detail. Section IV reports the experiment and presents a comparison of the results. Section V presents a discussion, and Section VI highlights the conclusion of this work and discusses future research.

II. ToF Measurement Algorithm and Sources of Error

TWR-based ToF measurement is the most accurate ranging algorithm for UWB, which is why it can be used as the basis for antenna delay calibration of UWB devices [9]. However, there are a number of sources of error that affect TWR's accuracy and precision in ranging, such as clock drifts and
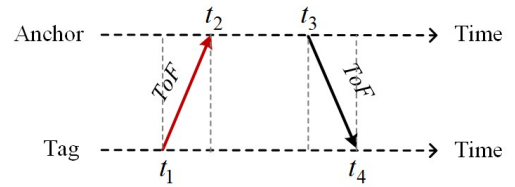

Fig. 1.   ToF algorithm principle.

frequency inconsistencies of devices [10]. It is necessary to eliminate or mitigate these errors before implementing the calibration. A short overview of the theory of the TWR protocol and the sources of error are introduced in detail in this section.

A. TWR Protocol

Two separated asynchronous devices can achieve ToF or distance measurement between each other by sending multiple communication messages and recording the corresponding timestamps (see Fig. 1). This method is also called single-side TWR (SS-TWR) [16].

t_1, t_4, t_3, and t_2 denote the recorded Tx and Rx timestamps of these messages at the tag/initiator side and the anchor/responder side, respectively. The ToF measurement can be determined by

$$\text{ToF} = 0.5 \cdot [(t_4 - t_1)\text{-}(t_3 - t_2)]. \tag{1}$$

Then, the distance between the tag and the anchor can be calculated by multiplying the speed of the radio signal in the air.

B. Sources of Error of TWR

Based on official application notes provided by Decawave [17], the main sources of error of TWR that affect the ranging accuracy and precision are the following: antenna Tx and Rx delays, clock drifts and frequency inconsistencies of the devices, and the received signal power level (RSL).

1) Antenna Tx and Rx Delays: Antenna Tx and Rx delays are internal to the UWB chip and are not included in the actual ToF measurement but in the propagation delay from the Tx timestamp to the Rx timestamp, as shown in Fig. 2(a). Then, the actual ToF between the tag and the anchor can be obtained by

$$\text{ToF}_{\text{measured}} = t_{\text{TX}} + \text{ToF}_{\text{actual}} + t_{\text{RX}}. \tag{2}$$

Fig. 2(b) shows an example of the measured ranging results of two DWM1001 modules at a distance of 0.5 m with respect to $t_{\text{TX}} = 0$ and $t_{\text{RX}} = 0$ for both devices. An offset of approximately 153.98 m is included in almost all the measurements, which cannot be neglected and accepted by any UWB-based applications.

Although the internal Tx and Rx delays of UWB chips vary slightly from chip to chip, the total delays in the propagation can vary for each device due to the distinctions of the external components between the UWB chip and the antenna. These variations cause differences in ranging measurements in the tens of centimeters, which is not acceptable, especially for
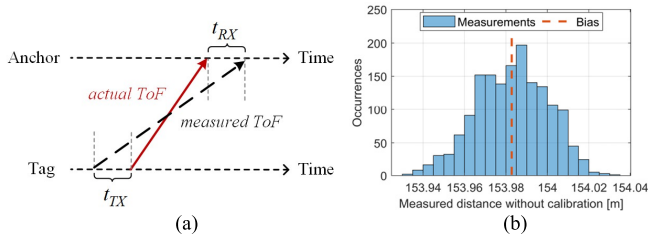
Fig. 2. Influence of the antenna delays of the tag and the anchor node on the measured ToF: (a) signals are not immediately transmitted and received at timestamping and (b) example of the measured ranging results at a distance of 0.5 m between the tag and the anchor without considering antenna delays; 1600 measured statistical results are included in (b).

Fig. 3. Example of the difference between the reply times of the tag and the anchor for AltDS-TWR.

high-accuracy UWB-based positioning systems. Therefore, antenna delay calibration is necessary for each UWB device to remove these variations.

2) Clock Drift and Frequency Errors of the Devices: For SS-TWR, a slight clock difference between the tag and the anchor can cause erroneous estimation of timestamps, resulting in inaccurate ToF measurements. The frequency errors of the crystal oscillator from its reference value on each device give rise to clock drift and therefore directly affect the accuracy of the timestamping process [17]. The effect of clock drifts on the ranging accuracy and precision can be mitigated by using an alternative double-side TWR (AltDS-TWR) algorithm since the ranging errors caused by clock drifts are dominated by the difference between the replay times of the tag and the anchor for AltDS-TWR [16]. For the DW1000 chip, we can precisely maintain the difference within 8 ns (one clock of the chip) using the integrated delay Tx function of the chip and the developed ranging method (see Section III), as shown in Fig. 3. Hence, the ranging errors caused by clock drifts could theoretically be less than 0.0015 cm considering a 20 ppm frequency error between the tag and the anchor [17]. The ranging errors caused by the frequency errors are dependent upon the replay time and the frequency drift of the ranging initiator for AltDS-TWR. The frequency drift of a room-temperature crystal oscillator is typically less than 0.05 ppm after the oscillator stabilizes, which corresponds to a ranging error of 0.75 cm with a reply time of 2 ms. Therefore, the total ranging errors caused by clock drifts and frequency errors could theoretically be less than 1 cm for AltDS-TWR. However, inaccurate timestamps recorded by UWB chips introduce extra random distance errors into the results, which is why AltDS-TWR can only achieve a ranging accuracy of less than approximately ±5 cm in actual measurements for the DW1000 chip, even in LoS conditions.

3) Received Signal Power Level: According to [17], a bias that varies with the RSL can be observed in the reported times-tamp of the received UWB signal, introducing a ranging bias in the evaluated ToF measurement. This bias can be ignored for most applications; however, higher precision ranging and positioning applications must correct it to ensure the performance of the applications. Although Decawave suggested a curve and an empirical lookup table in [17] where the bias corresponds to a specific RSL, and the relationship tends to
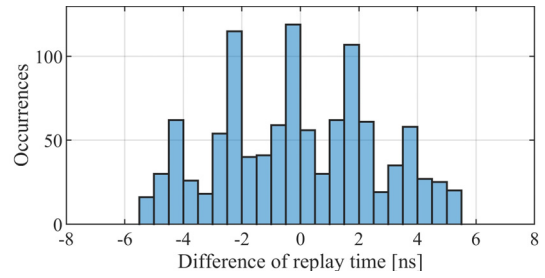
be linear, it is not practical to implement this approach in real environments because of the multipath effect of the radio frequency signals.

Based on the results presented in [18] and [21], although a highly nonlinear relationship may exist between the ToF measurement and the received signal level, especially the first path power level (FPL), it is difficult to fit it because any environmental noise, multipath or change in the environment affects the RSL and the correction accuracy. Some efforts have been made to address this case by applying machine learning or regression-based methods to predict distance errors, such as the Gaussian process regression-based method presented in [21]. However, complexity calculations in the training process heavily limit these methods from being used in actual applications, especially in applications with a large number of UWB devices. RSL-dependent distance errors are an interesting research topic but are outside the scope of this study, which is why we focus on the errors caused by the antenna delay and clock drift of the devices (trying to find easy methods to correct them to provide guidelines for actual UWB applications). The order of magnitude of the error due to the RSL could be larger than 10 cm, as shown by [17].

As mentioned above, RSL is another main factor that affects the ranging precision, resulting in an unexpected ranging bias in the measurements. This bias is caused by the inaccurate Rx timestamps estimated by the leading edge (LDE) algorithm [19] integrated into the UWB chips, which finds the "LDE" of the channel impulse response (CIR) of the received signals. The effect has been described and verified in [17] and [23]. Cano et al. [18] modeled these biases as a linear function of the FPL of the received signals. Although FPL is less sensitive to disturbances of multipath propagation than RSL, it is also less robust to the environment, even in LoS conditions, and can be easily affected by the environment. For example, the variation in FPL can be ±5 dBm when FPL is approximately −90 dBm based on the results of our experiments. Sidorenko et al. [20] tried to find the best signal power correction curves between the bias and the RSL by sending multimessages between the tag and the anchor. However, the correction curve is difficult to use in different scenarios due to the different multipath effects of the environments. Therefore, RSL- or FPL-based methods are not very suitable for actual applications. To avoid dependence on the RSL or FPL, Ledergerber and D'Andrea [21] and [22] proposed two effective methods to model and
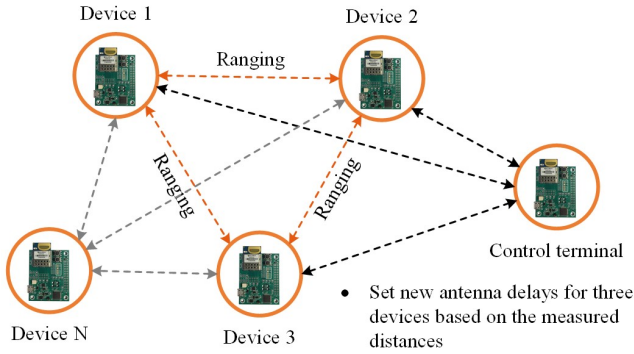
Fig. 4. Schematic of the proposed calibration.

correct the ranging biases using sparse pseudo-input Gaussian processes and a maximum likelihood approach. However, these methods strongly depend on the anchor setup and an extra angle measurement sensor is necessary for each UWB module. The distance pseudo measurements are deduced from the ToF measurements between the transceivers and depend on the accuracy of the angle sensor, thus consequently any measurement errors in the distance and angle estimations are fed back into the correction.

An optional method to correct the biases caused by RSL was presented by Flueratoru et al. [11]. A simple linear function was assumed between the measured distance and the true distance, which can be found by minimizing the squared error

$$E = \sum_{n=0}^{N} |x_n \cdot \rho_0 + \rho_1 - y_n|^2 \qquad (3)$$

where N, x_n, and y_n are the total number of measurements, the true distance, and the measured distance for all $n = 1, \ldots, N$, respectively. ρ_0 and ρ_1 are the polynomial coefficients to be evaluated. Although several caveats exist for the approach, as listed by Flueratoru et al. [11], this approach is efficient for correcting these ranging biases. Combined with the proposed antenna calibration method, it is possible to achieve a ranging accuracy within ± 5 cm for all distances and all anchor-tag pairs when all devices have the same hardware and configurations, and are calibrated at the same distance. Using a heterogeneous set of devices may have a detrimental impact on performance, and remains a quest for the future to achieve generality for the UWB positioning.

III. METHODOLOGY

Fig. 4 shows an overview of the proposed calibration, which is composed of four devices: three uncalibrated devices placed at the same distance and one control terminal. The control terminal is utilized to trigger the ranging between the devices and then estimate a new antenna delay set for the three devices based on the measured distances; thus the optimal delays for the three devices can be determined.

In addition, the calibration can be extended to N devices once the calibration for the first three devices is completed. The optimal delay of device N can be determined by averaging the estimated delays from the distances between device N and the three devices in the original set.

A. Message-Based Ranging Algorithm

Similarly, for the proposed approach, all the data used during the calibration are distance measurements. Therefore, a high-accuracy ranging algorithm is necessary to reduce the effect of distance errors on the calibration accuracy. As mentioned previously, AltDS-TWR is an optimal ranging method to address this case. It is an extension of the basic SS-TWR algorithm but is more accurate. Usually, the deviation of AltDS-TWR is less than 3 cm for UWBs in LoS conditions, which is sufficient for antenna delay calibration when we expect the calibration accuracy to be less than 10 cm or even 5 cm.

In addition, considering the actual case in which each UWB device has two independent Tx and Rx delays, each introduces bias into the ToF measurements. Although it is better to evaluate Tx and Rx delays independently, especially for high-accuracy applications, it is difficult to do so because both delays have equivalent effects on the ranking results. In addition, two pairs of unknown Tx and Rx delays exist for two UWB chips, but only two distance measurements can be obtained between them. There are not enough equations that can be constructed to evaluate them. To address this issue, a combined antenna delay T_* consisting of the Tx and Rx delay is typically used in the calibration, assuming the same Tx and Rx delay for each device. In this way, it is possible to evaluate all combined delays of the devices based on only the distance measurements among them. This method effectively reduces the complexity of the calibration without loss of accuracy based on the application notes provided by Decawave [9].

However, to realize this approach, it is necessary to ensure an equal number of Tx and Rx delays for each UWB device to reduce the effect of independent Tx and Rx delays on calibration accuracy. Although SS-TWR can address this case, the ranging accuracy of SS-TWR, usually ± 10 cm in LoS conditions, is not sufficient to ensure calibration accuracy. Instead, a four-message-based AltDS-TWR ranging algorithm (4M-AltDS-TWR) is implemented to measure the distance between the tag and anchor (see Fig. 5). There are two complete combined antenna delays for both the tag and anchor, thus; the effect of independent Tx and Rx delays on the calibration can be mitigated effectively. In addition, a request communication packet is also introduced into the ranging algorithm, as shown in Fig. 5. It can be used to ensure that the tag and the anchor have the same electrical status transforming from Tx to Rx or from Rx to Tx during the ranging process, reducing the random errors caused by the transformation. Similar to AltDS-TWR, 4M-AltDS-TWR can mitigate the ranging errors caused by the clock and frequency drifts of the devices based on the derivation presented in [16]. The measured ToF of 4M-AltDS-TWR can be obtained by

$$T_f = \frac{R_a R_b - D_a D_b}{R_a + D_a + R_b + D_b} \qquad (4a)$$

$$R_a = t_4 - t_1, \quad D_a = t_7 - t_6$$

$$R_b = t_8 - t_5, \quad D_b = t_3 - t_2. \qquad (4b)$$

The error included in (4a) can be modeled as

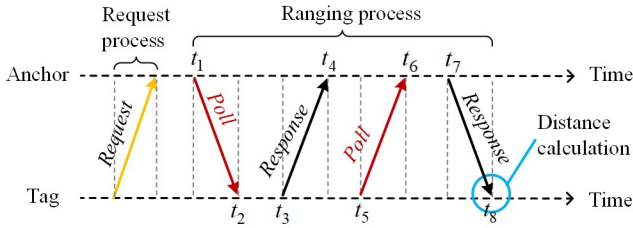$$T_f - \widetilde{T_f} = -e_1 \cdot T_f \text{ or } T_f - \widetilde{T_f} = -e_2 \cdot T_f \qquad (5)$$

Fig. 5. Message communicates in the 4M-AltDS-TWR method used for distance measurement between the tag and the anchor in this study.

Fig. 6. Flowchart of the approach.

where $T_f^{\sim}$ is the true ToF and e_1 and e_2 are the clock shift errors of the tag and the anchor, respectively. The detailed derivation process of (4) and (5) is given in the Appendix.

Using this scheme, the typical ranging errors caused by clock drifts could theoretically be in the low picosecond range even with a ±20 ppm crystal oscillator within a distance of 100 m. As a result, the error caused by clock shifts should be less than ±0.3 cm. Therefore, the inaccurate timestamps recorded by the UWB chips are the main factor affecting the ranging accuracy.

B. Antenna Delay Calibration

For UWB devices, the Tx and Rx delays change only slightly once the components between the UWB chip and the antenna have been soldered correctly in the devices [17]. Although changes in temperature introduce random errors to the measurements as well, these errors are extremely small. Therefore, the antenna delay is considered constant for each device. In this case, we can adjust the antenna delay of each UWB device within a certain range to determine the optimal value of the device by comparing the measured distance with the actual distance.

Fig. 6 shows an overview of the developed approach, which is composed of three major parts: initialization, coarse estimation, and fine-tuning estimation. Initialization is designed to determine inaccurate initial values for the three UWB devices involved in the calibration. Coarse estimation determines the same combined delay for three devices and ensures that the distance measurements between each pair of the three devices are within the expected tolerance. A two-way search-based approach (TWS) is developed to determine the optimal combined delay by dynamically adjusting the combined delays of the three UWB devices simultaneously and then determining the next possible candidate of the combined delay to be tested based on the measured distance and evaluated errors. Fine-tuning estimation determines the actual delay for each device by adjusting the antenna delays of the three devices slightly until the measured distances between each pair of the three devices match the actual distance as closely as possible.

Unexpected outliers may still appear in the results even with the developed 4M-AltDS-TWR algorithm. To remove the effect of outliers on the final calibration accuracy, a strategy that integrates a median filter is designed to detect and eliminate values that are larger than the specified median bounds during distance sampling (DS). The details of this strategy are described in Algorithm 1. By implementing this strategy, a certain amount of effective ToF measurements within the
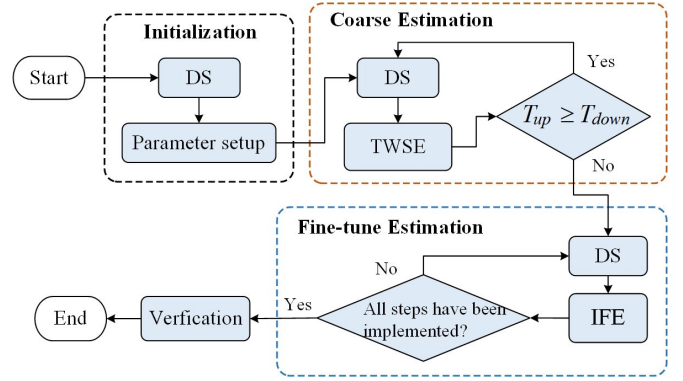
median bounds will be obtained. The median bounds were set to ±5 cm according to the ranging accuracy of the developed 4M-AltDS-TWR algorithm. The median of all the effective DSs is taken as the final value of the measurement between the tag and the anchor. All the distance measurements between each pair of the three devices within the initialization, coarse estimation, and fine-tuning estimation were implemented with this strategy to improve the ranging accuracy and thus improve the calibration accuracy.

Algorithm 1 DS

1: Set expected number N of the effective ToF measurements;
2: Obtain N 4M-AltDS-TWR measurements;
3: Sort the measurements and obtain the median d_{mean};
4: Filter out all the distances that are out of the median bounds and record the effective number M;
5: **While** $M < N$
6:     Obtain one 4M-AltDS-TWR measurement d;
7:     **If** $\|d - d_{mean}\| \leq 0.05$ m **do**
8:         $M = M + 1$;
9:         Record d as an effective measurement;
10:     **End**
11: **End**
12: Set distance to be the median of the samplings;

---

1) Initialization: In the initialization, first, we set all antenna delays of the three devices to zero. Then, we perform DS for each pair of the three devices and obtain the distance errors δ_{ij}, where $i \neq j$ and $i, j = 1, 2, 3$. Two dynamic variables are then set up to determine the upper-limit T_{up} and lower-limit T_{down} of the actual antenna delay T_{actual} of the three devices, which can be obtained by

$$T_{up} = \delta_d \cdot \xi + \Delta t \tag{6a}$$
$$T_{down} = \delta_d \cdot \xi - \Delta t \tag{6b}$$

where ξ is a factor used to transform the measured distance to the UWB chip time, δ_d denotes the maximum value of δ_{ij}, and Δt is a constant used to determine the search scope of the coarse estimation. The difference in the combined antenna delays between different UWB devices is typically less than 10 ns or 3 m in distance, especially for devices composed

of the same UWB chip and the same external components based on our tests. In this case, we set $\Delta t = 500$, which corresponds to an adjustment range of approximately 4.7 m. This is definitely sufficient for the calibration. Finally, the combined delay is set to be the mean T_{mean} of the two limits for each device.

2) Coarse Estimation: As mentioned previously, coarse estimation was implemented to determine the same combined antenna delay for the three devices, and TWS was applied to determine the new values of the upper limit T_{up} and lower limit T_{down} and thus the final combined delay of the three devices. The details of TWS are presented in Algorithm 2. First, DS is performed for each pair of the three devices; thus, six measured distances d_{ij}, where $i \neq j$, can be obtained. Based on these measurements, a score factor used to determine the adjustment direction of the two limits can be calculated by

$$\delta = \begin{cases} \delta + 1, & \text{if } d_{ij} - d_{\text{actual}} < 0 \\ \delta - 1, & \text{if } d_{ij} - d_{\text{actual}} > 0. \end{cases} \tag{7}$$

Algorithm 2 TWS

1: **While** $T_{down} < T_{up}$
2:     Set delays to $T = (T_{up} + T_{down})/2$ for each device;
3:     Do DS for each pair of devices and obtain the ranging errors δ_{ij};
4:     Obtain direction factor δ by solving Formula (7);
5:     Set new value for T_{up} or T_{down};
6:     $T'_{up} = T, if\, \delta > 0$ or $T'_{down} = T, if\, \delta < 0$;
7:     **If** $\delta = 0$ **do**
8:         Obtain the fine-tuning factor by solving Formula (8);
9:         Obtain new values for T_{up} and T_{down};
10:         $T'_{up} = T_{up} - T_{ft}$, $T'_{down} = T_{down} + T_{ft}$;
11:     **End**
12:     $\delta = 0$;
13:     Update T_{up} and T_{down};
14: **End**
15: Set combined delay to $T = (T_{up} + T_{down})/2$ for each device;

In the early stages of the coarse estimation, the evaluated combined delay is always too far from the actual value; thus, the factor δ is always larger or smaller than zero. In these cases, the new values of the upper limit and lower limit can be determined easily with $T'_{\text{up}} = T_{\text{mean}}, \text{if} \delta < 0$ and $T'_{\text{down}} = T_{\text{mean}}, \text{if} \delta < 0$, where T_{mean} denotes the median of the old upper limit and lower limit. However, the evaluated combined delay will approach the actual value, as the adjustment proceeds smoothly. As a result, the score factor δ becomes more random especially in the later process of the estimation, due to the ranging errors of the 4M-AltDS-TWR algorithm, as shown in Fig. 7. In this case, it is inaccurate to determine the new upper limit and lower limit only with T_{mean} and δ. To address this issue, a fine-tuning factor T_{ft} is introduced to decelerate the estimation process, which can be obtained by

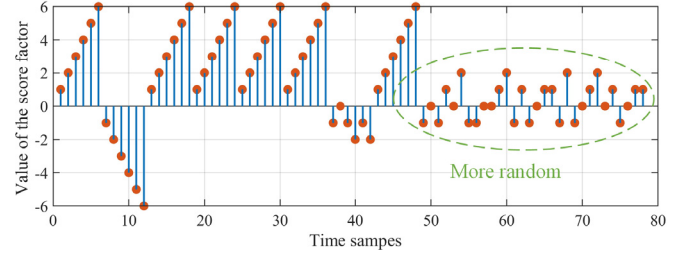$$T_{\text{ft}} = (T_{\text{up}} - T_{\text{down}}) \cdot \alpha \tag{8}$$

Fig. 7. Example of the variation in the factor δ in the coarse estimation.

where $\alpha = 0.2$ is a fixed factor used to obtain T_{ft}. α can also be set to other values to increase or decrease the coarse estimation. Then, the new upper limit and lower limit can be determined by the factor T_{ft}, as shown in Algorithm 2. The complexity of TWS is approximately equal to $\Theta(\log_2 n)$ because its core is based on a binary search algorithm, where n is the search scope of the initialized upper limit and lower limit. The corresponding time consumption of TWS for the UWB device is $\Theta(\log_2 n) \cdot t_{\text{DS}}$, where t_{DS} is the total sampling time of DS.

3) Fine-Tuning Estimation: After the coarse estimation, the combined delay should be the same for all three devices, but the actual delay can vary for each device due to the distinctions of the external components between the UWB chip and the antenna, such as the balun, as well as the difference in the power system of the device. For high-accuracy applications, these variations must be calibrated carefully for each UWB device to ensure the performance of the positioning system.

To determine the actual value of these variations for each UWB device, an iterative-based fine-tuning (IFE) estimation algorithm is introduced, as shown in Algorithm 3. Fig. 8 describes the structure of the IFE. The combined antenna delays of the three devices are adjusted one by one in the IFE, and the best values with the minimum distance errors are recorded during the estimation. In this way, the optimal set of delays can be found once all the expected steps have been implemented by the three devices. Two factors are designed to determine the distance errors, as shown in (9). One is based on the errors between the measured distance and the actual distance, and the other is based on the errors between all the measured distances

$$\sigma_1 = \sum_{i,j}^{i \neq j} |d_{ij} - d| \tag{9a}$$

$$\sigma_2 = \sum_{i,j}^{i \neq j} |d_{ij} - R|, \quad R = \{d_{ij}\}|i \neq j. \tag{9b}$$

These two errors should be as close as possible to zero because all the measured distances should theoretically be equal to the designed calibration distance. In this case, the best set of delays of the three devices can be determined by recording the minimum of the two errors

$$[T_1, T_2, T_3] = \min\{\sigma_1, \sigma_2\}. \tag{10}$$

In addition, we used undulating steps with a uniform distribution to conduct the adjustment set, as shown in Algorithm 3,
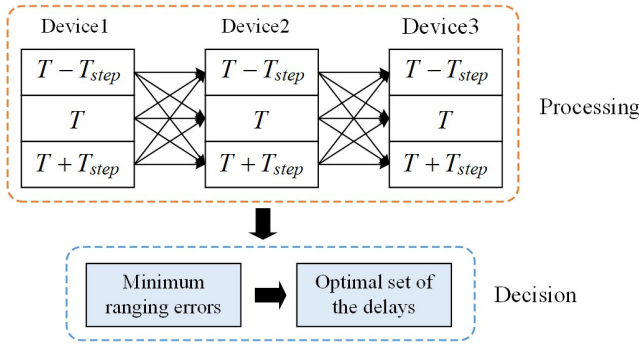
Fig. 8.   Structure of IFE.

Algorithm 3 IFE

1: **If** combined delay T of coarse estimation is an odd number **do**
2:　　　　　Set　adjustment　set　to
　　$T_{step} = [2, 4, 6, 8, 10, 12, 2, 4, 6, 8, 10, 12] \cdot T_{UWB}$;
3: **else**
4:　　　　　Set　adjustment　set　to
　　$T_{step} = [1, 3, 5, 7, 9, 11, 1, 3, 5, 7, 9, 11] \cdot T_{UWB}$;
5: **End**
6: **repeat**
7:　**for** $T_1 \pm T_{step,i}$, $T_2 \pm T_{step,i}$ and $T_3 \pm T_{step,i}$ **do**
8:　　Set antenna delays;
9:　　Perform DS for each pair of the three devices;
10:　　Calculate ranging errors σ_1 and σ_2 by solving Formula (9);
11:　　Record T_1, T_2 and T_3 with minimum σ_1 and σ_2;
12:　**End**
13: **until** all the steps have been implemented by the three devices;

---

which is beneficial for improving the estimation accuracy. Different sets composed of odd numbers or even numbers were applied for different results of coarse estimation to ensure that all new values of Tx and Rx antenna delay to be evaluated could be different from the old measured value. T_{UWB} denotes the unit time of the UWB chip. For DW1000, it corresponds to a distance of approximately 0.0047 m. Therefore, IFE can fulfill an adjustment range of approximately 0.17 m for three devices, which is sufficient for fine-tuning calibration. Moreover, the time consumption of IFE is $N^3 \cdot t_{DS}$, where N and t_{DS} are the number of steps and the total sampling time of DS, respectively.

IV. EXPERIMENTAL RESULTS

To verify the performance of TWS and IFE, enrichment experiments were implemented in a typical office space of $7 \times 9 \times 2.6$ m at the Finnish Geospatial Research Institute (FGI), as shown in Fig. 9. Three MDEK1001 kits containing DW1000 chips were used in these experiments, and Table I shows the parameters used. The target distance and the power at the received input were set to 5.01 m and -104 dBm/MHz, respectively, based on the recommended value of the DW1000 manual. LoS conditions were maintained for the three devices at all times. DS was implemented to perform a range between

TABLE I
PARAMETERS OF THE DW1000 CHIP USED IN ALL THE EXPERIMENTS

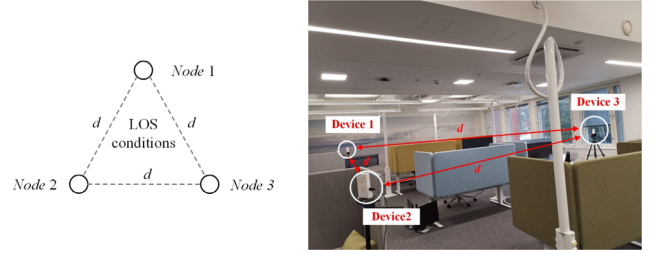| Parameter	Channel	PRF	Preamble Length	Data Rate
Values	5	64 MHz	256	6.8 Mbps

Fig. 9.   Experimental layout of antenna delay calibration. Three uncalibrated UWB devices were placed at the same known distance from each other. During the calibration process, LoS conditions were maintained for the three devices at all times. An equilateral triangle was used in these experiments so that the treatment of the range bias in the calculation is simplified because the range bias should be the same for the three devices with the same distance between each other [9].

the devices, and the sampling number was set to 10 to accelerate the estimation for both TWS and IFE. The total time consumption of DS was approximately 0.1 s, which can be obtained by $t = 6M \cdot t_{\text{4M-AltDS-TWR}}$, where M and $t_{\text{4M-AltDS-TWR}}$ are the sampling number of DS and the time consumption of each 4M-AltDS-TWR range, respectively. One of the three devices was connected to a PC to collect the raw measured distances, debug information, and the final calibrated delays. The calibrated combined delays were also recorded in the OTP memory of the UWB chip and the flash memory of the microprocessor; thus, the devices can use them directly in actual applications. Therefore, the calibration was real-time and automatic, which is significant for practical applications.

In addition, multiple tests, marked as Test-1–Test-3, were implemented to verify the reliability of TWS and IFE, in which the test configuration remains the same, e.g., set t_{TX} and t_{RX} to zero for all the devices at the start of the calibration. Furthermore, an extra test, marked as Test-4, was implemented to verify the robustness of the TWS and IFE by exchanging the device number between Devices 2 and 3.

Table II shows the evaluated combined delays of the three devices in different tests, as well as Decawave's measured results. Fig. 10 shows a comparison of the distribution of the distance errors of TWS and IFE of Test-1, computed as

$$e_d = d' - d \tag{11}$$

where d' is the measured distance and d is the true distance. The results of Test-2, Test-3, and Test-4 are very close to those of Test-1 because there is little difference between the obtained combined delays. Thus, the distributions of the distance errors of these tests are not presented in this section. Fig. 11 shows the corresponding cumulative distribution function (cdf) of the total distance errors of the IFE in different tests.

Based on the results in Table II, Figs. 10 and 11, it can be seen that TWS and ISE achieve calibration accuracies of better than approximately ± 0.06 m and even better than ± 0.01 m for each device, respectively. Although slight differences exist for

TABLE II
COMBINED DELAYS OF THREE DEVICES

Items		Device1	Device2	Device3
Test-1	TWS	32870	32870	32870
	IFE	**32860**	**32858**	**32888**
Test-2	TWS	32875	32875	32875
	IFE	**32857**	**32857**	**32889**
Test-3	TWS	32873	32873	32873
	IFE	**32865**	**32861**	**32881**
Test-4	TWS	32867	32867	32867
	IFE	**32859**	**32865**	**32881**
Decawave's results		**32918**	**32916**	**32914**
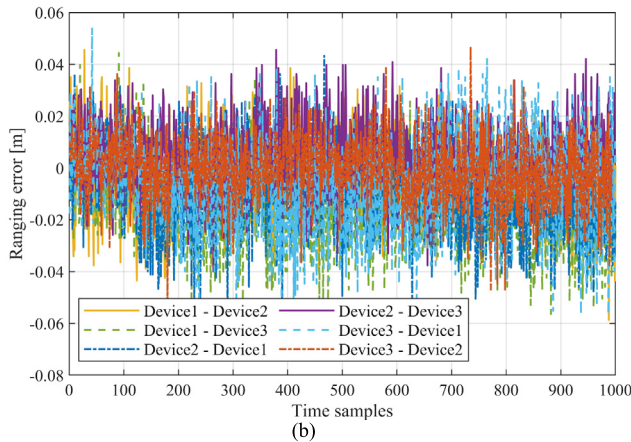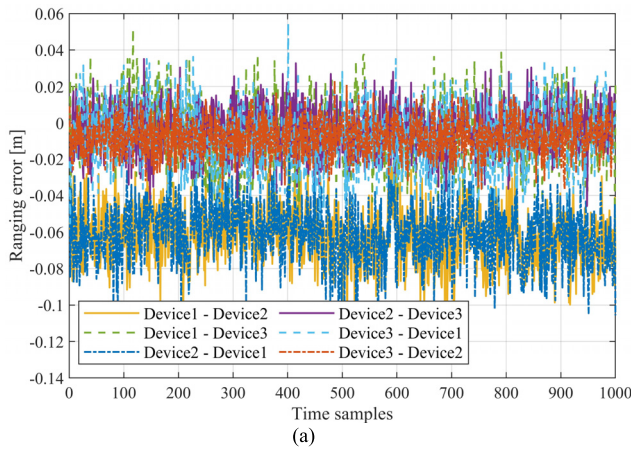
Fig. 10. Distribution of distance errors of (a) TWS and (b) IFE in Test-1.
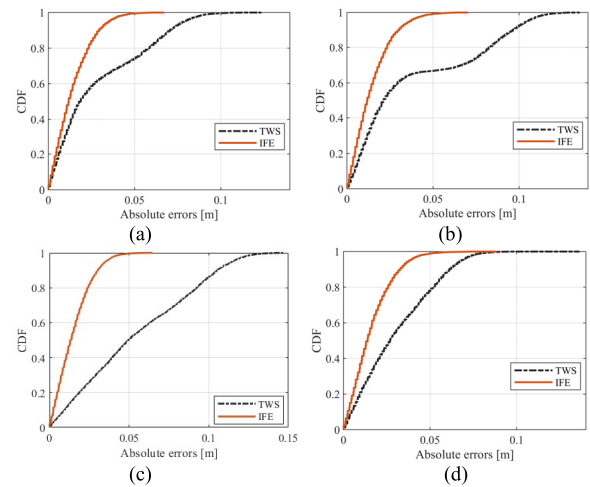

Fig. 11. CDF of the total distance errors of different tests. (a) Test-1. (b) Test-2. (c) Test-3. (d) Test-4.

TABLE III
STATISTICS OF THE DISTANCE ERRORS

Method	Distance [m]	Mean [m]	Standard deviation [m]	IQR [m]
Decawave	1	0.24	0.02	0.47
	3,5,7,9	0.07	0.03	0.14
TWS-IFE	1	0.09	0.01	0.18
	3,5,7,9	0.02	0.01	0.03

different tests, especially in the final combined delays, TWS and ISE demonstrate extreme reliability and robustness. The differences in the final combined delays from Test-1 to Test-3 are almost within 10 units of the UWB time or a distance of approximately 5 cm. They are exactly the ranging precision of the 4M-AltDS-TWR method. Therefore, more precise ranging methods can be developed to further improve the calibration accuracy, which is one of the main research points for future work.

To verify the ranging accuracy and precision of the developed antenna delay calibration method at different distances, we used two of the calibrated devices to further perform ranging tests in the same office space. Four test points with different distances, 1, 3, 7, and 9 m, were selected. A total of 2000 distance measurements were obtained for each test point. Table III shows the mean, standard deviation, maximum and interquartile range (IQR) of the errors, computed based on (11). The results for the test point at a distance of 1 m are listed individually, considering the case that a larger received signal level will be included at both the transmitter and receiver sides, resulting in a larger ranging bias. Fig. 12 compares the individual distribution of the distance errors of the proposed TWS-IFE and Decawave's method, and Fig. 13 shows a histogram of the absolute errors, as well as the corresponding cdf.

The results show that TWS-IFE has a smaller bias and better-ranging precision than Decawave's method because most of the results of TWS-IFE are less than ±0.05 m when the distance is greater than 3 m. In addition, for TWS-IFE, the mean and standard deviation of the distance errors even reach 0.01 m when the distance is larger than 1 m. All these results show that TWS-IFE has excellent accuracy and precision compared to Decawave's benchmark method. In addition, the distance errors at 1 m, approximately 0.1 m for TWS-IFE and 0.24 m for Decawave's benchmark method, are obviously larger than other tested distances for both methods, which is caused mainly by the extreme RSL and FPL of the UWB pulse at a close distance, resulting in a larger negative ranging bias. Therefore, antenna calibration should be implemented with a correct parameter setup in terms of the distance and the signal power level.
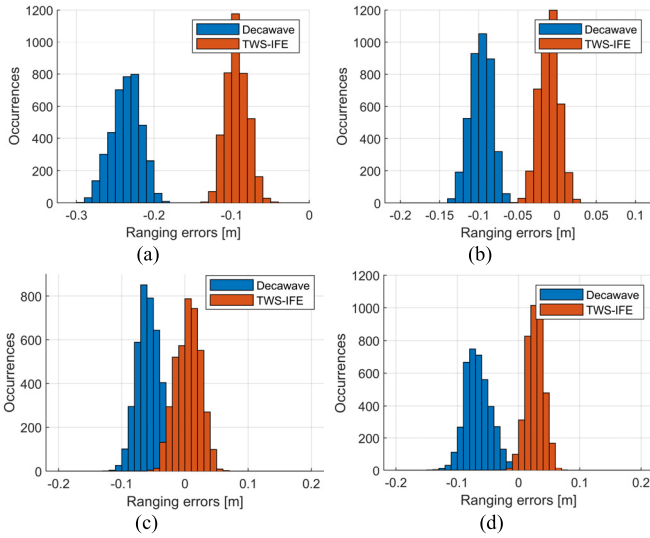
Fig. 12. Comparison of the distribution of aggregated distance errors. (a) Distance at 1 m. (b) Distance at 3 m. (c) Distance at 7 m. (d) Distance at 9 m.
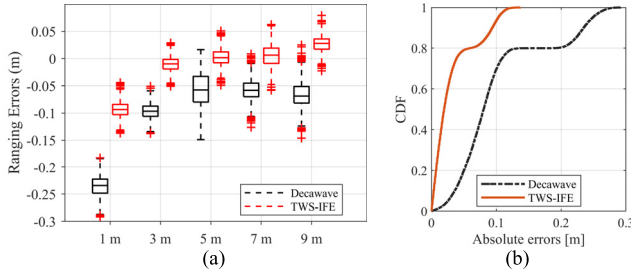

Fig. 13. Statistical results of the distance errors, (a) individual distribution of the distance errors of different tested points, and (b) cdf of the total distance errors.
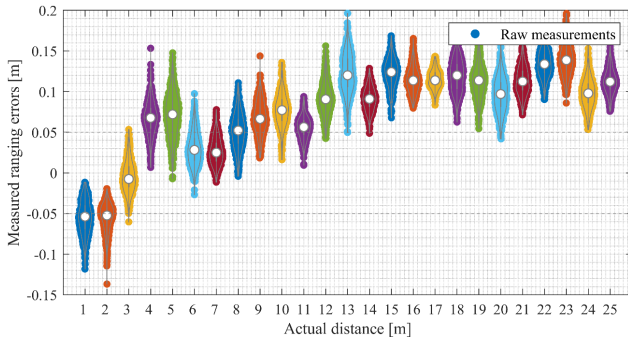

Fig. 14. Outdoor scenarios, keeping LoS conditions between the tag and the anchor at all times during the tests.

In addition, an outdoor test was performed to verify the ranging accuracy and precision for a larger distance range from 1 to 25 m. Two calibrated devices (one tag and one anchor) deployed on a tripod with a height of approximately 1.4 m to the ground were used to perform the test. LoS conditions were maintained between the tag and the anchor at all times during the test. Five hundred distance measurements were obtained at the tag side for each tested distance. Fig. 14 shows the estimated ranging errors. The results show that an average ranging precision of less than approximately ±12 cm
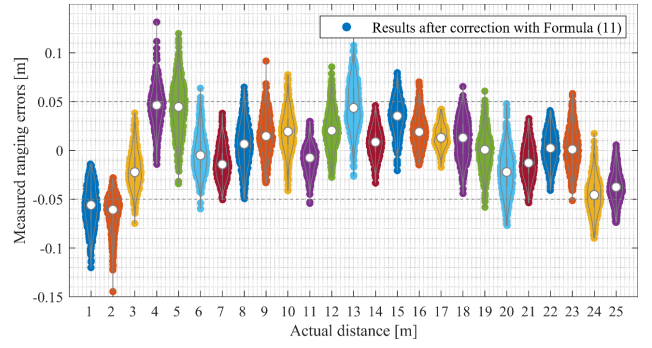

Fig. 15. Ranging errors of the calibrated measurements.

was achieved by the proposed calibration for all the tested distance ranges. Furthermore, the ranging precision increased to approximately 12 cm when the tested distance exceeded 12 m, and different biases are included for these distances, which are mainly caused by different RSLs, as mentioned in Section II. This effect can be corrected further by modeling the relationship between the bias and the distance, as presented in Section II. Fig. 15 shows the corresponding results after the correction. The average ranging precision decreases to less than ±5 cm, improving by 58.3%.

V. CONCLUSION

This article developed a real-time and fully automatic antenna delay calibration approach that can easily be utilized to evaluate the combined antenna delay of each individual/single UWB device used in a positioning system. In contrast to traditional approaches, more precise calibration results and more efficient implementation are obtained. When implementing the TWS-based coarse estimation, the same combined delay is obtained for all three devices. Then, more accurate estimation values are obtained for each device by continuously implementing the IFE-based fine-tuning estimation. The developed approach was verified to achieve a ranging precision of better than ±0.01 m within a base UWB network for each pair of devices and achieves a ranging accuracy and precision of better than ±0.05 m in a distance range from 1 to 25 m after calibration and bias correction for a remote/moving UWB, making it an optimal solution for UWB positioning applications. In addition, all parts of the approach can be performed in real-time, making it extremely useful for UWB applications in the real world.

For UWB-based positioning systems, in addition to antenna delay, RSL is a major factor affecting ToF estimation accuracy and thus the system positioning accuracy. It is worth looking into in the future. Meanwhile, how determining the Tx and Rx delay of each device independently would be a significant feat to achieve more precise ranging and positioning with UWB.

APPENDIX
4M-ALTDS-TWR

Let T_f denotes the actual ToF of the wideband pulse signals traveling between a tag and an anchor, R_a and D_a denote the

replay time and delay time of the anchor in the 4M-AltDS-TWR, and R_b and D_b denote the replay time and delay time of the tag in the 4M-AltDS-TWR, respectively. It is clear that with ideal time references, R_a and R_b can be obtained by

$$R_a = t_4 - t_1 = 2T_f + D_b \tag{12a}$$

$$R_b = t_8 - t_5 = 2T_f + D_a \tag{12b}$$

where $D_a = t_7 - t_6$ and $D_b = t_3 - t_2$.

Multiplying both equations in (12), we can get

$$R_a R_b = (2T_f + D_b)(2T_f + D_a) \tag{13}$$

which can easily be expanded and rearranged to obtain

$$R_a R_b - D_a D_b = 2T_f(2T_f + D_a + D_b). \tag{14}$$

From (12) and (14), we can rewrite (14) as (15a) and (15b) by replacing the appropriate terms

$$R_a R_b - D_a D_b = 2T_f(R_a + D_a) \tag{15a}$$

$$R_a R_b - D_a D_b = 2T_f(R_b + D_b). \tag{15b}$$

Finally, T_f can be obtained by

$$T_f = \frac{R_a R_b - D_a D_b}{2(R_a + D_a)} = \frac{R_a R_b - D_a D_b}{2(R_b + D_b)}. \tag{16}$$

Based on [16], (12) and (15) imply that $R_a + D_a$ equals $R_b + D_b$, and it is easy to achieve this in 4M-AltDS-TWR, thus (16) could also be written as

$$T_f = \frac{R_a R_b - D_a D_b}{R_a + D_a + R_b + D_b}. \tag{17}$$

Here, we assume that the clock drift of the device is the dominant source of errors affecting the ToF measurement, the clock drift of R_a, D_a, R_b, and D_b can then be modeled as

$$R_a^\sim = (1 + e_a)R_a = k_a R_a, \quad D_a^\sim = (1 + e_a)D_a = k_a D_a \tag{18a}$$

$$R_b^\sim = (1 + e_b)R_b = k_b R_b, \quad D_b^\sim = (1 + e_b)D_b = k_b D_b \tag{18b}$$

where e_a and e_b are the clock shift errors of the anchor and tag.

Combining (16) and (18), the true value of T_f can be obtained by

$$T_f^\sim = \frac{k_a k_b}{k_a} \frac{R_a R_b - D_a D_b}{2(R_a + D_a)} = k_b T_f$$

$$= \frac{k_a k_b}{k_b} \frac{R_a R_b - D_a D_b}{2(R_b + D_b)} = k_a T_f. \tag{19}$$

Therefore, the ToF error is

$$T_f - T_f^\sim = T_f - k_a T_f = -e_a T_f$$

$$= T_f - k_b T_f = -e_b T_f. \tag{20}$$

REFERENCES

[1] J. Wang, R. K. Ghosh, and S. K. Das, "A survey on sensor localization," *J. Control Theory Appl.*, vol. 8, no. 1, pp. 2–11, 2010.

[2] R. Mautz, "Indoor positioning technologies," Habilitation thesis, Dept. Civil, Environ. Geomatic Eng., Inst. Geodesy Photogramm., ETH Zürich, Zürich, Switzerland, 2012.

[3] W. Sakpere, M. A. Oshin, and N. B. Mlitwa, "A state-of-the-art survey of indoor positioning and navigation systems and technologies," *South Afr. Comput. J.*, vol. 29, no. 3, pp. 145–197, Dec. 2017.

[4] R. Chen et al., "Precise indoor positioning based on acoustic ranging in smartphone," *IEEE Trans. Instrum. Meas.*, vol. 70, pp. 1–12, 2021.

[5] Z. Liu, R. Chen, F. Ye, G. Guo, Z. Li, and L. Qian, "Improved TOA estimation method for acoustic ranging in a reverberant environment," *IEEE Sensors J.*, vol. 22, no. 6, pp. 4844–4852, Mar. 2022.

[6] J. Tiemann and C. Wietfeld, "Scalability, real-time capabilities, and energy efficiency in ultra-wideband localization," *IEEE Trans. Ind. Informat.*, vol. 15, no. 12, pp. 6313–6321, Dec. 2019.

[7] F. Mazhar, M. G. Khan, and B. Sällberg, "Precise indoor positioning using UWB: A review of methods, algorithms and implementations," *Wireless Pers. Commun.*, vol. 97, no. 3, pp. 4467–4491, Dec. 2017.

[8] D. Yang, A. E. Fathy, H. Li, M. Mahfouz, and G. D. Peterson, "Millimeter accuracy UWB positioning system using sequential sub-sampler and time difference estimation algorithm," in *Proc. IEEE Radio Wireless Symp. (RWS)*, Jan. 2010, pp. 539–542.

[9] (2018). *APS014 Application Note, Antenna Delay Calibration of DW1000-Based Products and Systems*. Decawave, Dublin, Ireland. [Online]. Available: https://www.decawave.com/application-notes/

[10] C. Lian Sang, M. Adams, T. Hörmann, M. Hesse, M. Porrmann, and U. Rückert, "Numerical and experimental evaluation of error estimation for two-way ranging methods," *Sensors*, vol. 19, no. 3, p. 616, Feb. 2019.

[11] L. Flueratoru, S. Wehrli, M. Magno, E. S. Lohan, and D. Niculescu, "High-accuracy ranging and localization with ultrawideband communications for energy-constrained devices," *IEEE Internet Things J.*, vol. 9, no. 10, pp. 7463–7480, May 2022.

[12] A. Basiri et al., "Indoor location based services challenges, requirements and usability of current solutions," *Comput. Sci. Rev.*, vol. 24, pp. 1–12, May 2017.

[13] K. A. Horváth, G. Ill, and Á. Milánkovich, "Calibration method of antenna delays for UWB-based localization systems," in *Proc. IEEE 17th Int. Conf. Ubiquitous Wireless Broadband (ICUWB)*, Sep. 2017, pp. 1–5.

[14] X. Gui, S. Guo, Q. Chen, and L. Han, "A new calibration method of UWB antenna delay based on the ADS-TWR," in *Proc. 37th Chin. Control Conf. (CCC)*, Jul. 2018, pp. 7364–7369.

[15] S. Shah, K. Chaiwong, L.-O. Kovavisaruch, K. Kaemarungsi, and T. Demeechai, "Antenna delay calibration of UWB nodes," *IEEE Access*, vol. 9, pp. 63294–63305, 2021.

[16] D. Neirynck, E. Luk, and M. McLaughlin, "An alternative double-sided two-way ranging method," in *Proc. 13th Workshop Positioning, Navigat. Commun. (WPNC)*, Oct. 2016, pp. 1–4.

[17] *Decawave, Sources of Error in DW1000 Based Two-Way Ranging (TWR) Schemes, Application Note, Version 1.1*, Decawave, Dublin, Ireland, 2014.

[18] J. Cano, G. Pagès, É. Chaumette, and J. LeNy, "Clock and power-induced bias correction for UWB time-of-flight measurements," *IEEE Robot. Autom. Lett.*, vol. 7, no. 2, pp. 2431–2438, Apr. 2022.

[19] I. Sharp, K. Yu, and Y. J. Guo, "Peak and leading-edge detection for time-of-arrival estimation in band-limited positioning systems," *IET Commun.*, vol. 3, no. 10, pp. 1616–1627, 2009.

[20] J. Sidorenko, V. Schatz, N. Scherer-Negenborn, M. Arens, and U. Hugentobler, "Decawave UWB clock drift correction and power self-calibration," *Sensors*, vol. 19, no. 13, p. 2942, Jul. 2019.

[21] A. Ledergerber and R. D'Andrea, "Ultra-wideband range measurement model with Gaussian processes," in *Proc. IEEE Conf. Control Technol. Appl. (CCTA)*, Kohala Coast, HI, USA, Aug. 2017, pp. 1929–1934.

[22] A. Ledergerber and R. D'andrea, "Calibrating away inaccuracies in ultra wideband range measurements: A maximum likelihood approach," *IEEE Access*, vol. 6, pp. 78719–78730, 2018.

[23] F. Che et al., "Feature-based generalized Gaussian distribution method for NLoS detection in ultra-wideband (UWB) indoor positioning system," *IEEE Sensors J.*, vol. 22, no. 19, pp. 18726–18739, Oct. 2022.

Zuoya Liu is currently a Post-Doctoral Researcher at the Department of Remote Sensing and Photogrammetry, Finnish Geospatial Research Institute, Espoo, Finland. His research interests include positioning and navigation technologies, wireless networks, multisensor cooperative control, signal processing, the Internet of Things, and forest surveying.

Teemu Hakala is currently an Academic Researcher at the Department of Remote Sensing and Photogrammetry, Finnish Geospatial Research Institute, Espoo, Finland. He has contributed to research in topics: terrestrial, mobile, and airborne laser scanning, spectrometry, hyperspectral imaging and lidar, drone, and forest health.

Juha Hyyppä is currently a Professor and the Director of the Department of Remote Sensing and Photogrammetry, Finnish Geospatial Research Institute, Espoo, Finland. His research interests include laser scanning systems, their performance, and new applications, especially related to mobile and ubiquitous laser scanning systems including autonomous driving, and point cloud processing.

Antero Kukko is currently a Professor at the Department of Remote Sensing and Photogrammetry, Finnish Geospatial Research Institute, Espoo, Finland. His expertise comprises a variety of aspects of laser scanning and image data, including both system developments and data processing for mobile and airborne laser scanning, and research and development of automatic image registration methods.

Harri Kaartinen is currently a Research Professor at the Department of Remote Sensing and Photogrammetry, Finnish Geospatial Research Institute, Espoo, Finland. He coordinates and conducts research on performance and quality issues related to laser scanning sensors, systems, and applications, with abundant skills and expertise in GNSS, geomatic, laser scanning, mapping, and remote sensing.

Ruizhi Chen is currently a Professor of the State Key Laboratory of Information Engineering in Surveying, Mapping and Remote Sensing, Wuhan University, Wuhan, China, and an Academician of the Finnish Academy of Science and Letters, Helsinki, Finland. He is committed to theoretical research and core technology development for seamless indoor/outdoor positioning using smartphones.